Recalibration of the Intensity Prediction Equation in Italy Using the Macroseismic Dataset DBMI15 Version 2.0

Recalibration of the intensity prediction equation in Italy using the Macroseismic Dataset DBMI15 V2.0

Lolli[1] B., Gasperini[2,1] P., Vannucci[2] G.

[1]Istituto Nazionale di Geofisica e Vulcanologia, Sezione di Bologna

[2]Dipartimento di Fisica e Astronomia, Università di Bologna

Abstract

We re-compute the coefficients of the intensity prediction equation (IPE) in Italy using the data of the DBMI15 V2.0 intensity database and the instrumental and combined (instrumental plus macroseismic) magnitudes reported by the CPTI15 V2.0 catalog. We follow the same procedure described in a previous article, consisting of a first step in which the attenuation of intensity I with respect to the distance D from macroseismic hypocenter is referred to the expected intensity at the epicenter I_E and a second step in which I_E is related to the instrumental magnitude M_i, the combined magnitude M_c, the epicentral intensity I_0 and the maximum intensity I_{max}, using error-in-variable (EIV) regression methods.

The main methodological difference with respect to the original article concerns the estimation of the uncertainty of I_E to be used for EIV regressions, which is empirically derived from the standard deviation of regression between I_E and M_i and also used for the regressions of I_E with M_c, I_0 and I_{max}.

In summary, the new IPE determined from DBMI15 V2.0 is

$$I = I_E - 0.0081(D - h) - 1.072[\ln(D) - \ln(h)]$$

where $D = \sqrt{R^2 + h^2}$, h=4.49 km and I_E can be calculated from the intensity data distribution of the earthquake. If the intensity data distribution is not available, I_E can be calculated from the following relationships

$$I_E = -2.578 + 1.867M_w$$

$$I_E = I_0$$

Introduction

The ground motion prediction equation (GMPE), also called ground motion model (GMM), describing the attenuation of the amplitude of ground shaking and the associated standard deviation as a function of several explanatory variables, i.e., magnitude, distance, site conditions, style of faulting and other parameters, is one of the basic ingredients of seismic hazard assessment (e.g. Cornell, 1968). Usually, seismic hazard is expressed in terms of physical quantities like the peak ground acceleration (PGA) or the spectral ordinates at different frequencies of such physical quantity. However, spectral acceleration, and particularly PGA, is weakly related to earthquake damage (Wald et al., 1999; Atkinson and Kaka, 2007), hence, seismic hazard is sometimes expressed in terms of macroseismic intensity (McGuire, 1993), especially in countries like Italy (Albarello et al., 2002, Gómez Capera et al., 2010) where a large intensity database is available. In this case the GMPE (or GMM) becomes an intensity prediction equation (IPE).

In principle, macroseismic intensity is only an ordinal (integer) classification of effects produced by earthquakes on humans, buildings and the environment, not physically related to the amplitude of the ground motion. However, based on the works of Cancani (1904) and Sieberg (1912, 1932), the Mercalli Cancani Sieberg (MCS) intensity scale and its successors up to the latest European Macroseismic Scale (Grünthal, 1998) were designed so that each degree of the scale corresponds to a level of ground motion which is about twice than that of the previous degree. Note that the accelerations reported by Cancani (1904) were not directly measured by instruments, which were not available at the time, but rather inferred by other kind of observations like the potential shifting of objects of different weight. This implies a logarithmic relationship between intensity and ground motion amplitude which has been confirmed empirically by several studies (e.g. Wald et al., 1999, Tselentis and Danciu, 2008,

62 Faenza and Michelini, 2010, Zanini et al., 2019, Gomez-Capera et al., 2020, Oliveti et al.,
63 2022).
64 Pasolini et al. (2008b) proposed a two-step procedure for deriving the IPE in Italy based on the
65 Data Base of Macroseismic Intensity, Version 2004 (DBMI04, Stucchi et al., 2007). The latter
66 was including more than 58000 Macroseismic Data Points (MDPs) but based on various quality
67 criteria, Pasolini et al. (2008b) selected about 22500 of them to be fitted by a log linear
68 regression law with the distance from the macroseismic hypocenter (assuming a constant depth
69 for all earthquakes). In the course of time, the Italian macroseismic database definitely
70 improved, up to include more than 120000 MDPs in the DBMI V2.0 (Locati et al., 2019). In
71 this work we apply the same procedure by Pasolini et al. (2008b) to such more recent data.
72 We did not use the latest versions (V3.0 and V4.0) of the DBMI15 dataset (Locati et al., 2021,
73 2022), which became available during the preparation of the present work, because the effort
74 needed to redo all the computations was not justified by the small number of changes with
75 respect to V2.0. In fact, such changes only concern a few small earthquakes: 7 from 2019 to
76 2020 and 6 in Sicily from 2014 to 2017, for a total of 226 MDPs added (see table S3 and S4 in
77 the Supplemental Material).
78 A preliminary version the present study (Lolli et al., 2019) was produced within the ambit of
79 the revaluation of the Italian seismic hazard map MPS19 (Meletti et al., 2021).
80
81 **Application of the Pasolini et al. (2008b) procedure**
82
83 The procedure described by Pasolini et al. (2008b) consists of two steps: in the first one, the
84 attenuation of intensity I with respect to hypocentral distance D is referred to the "expected
85 intensity at the epicenter" I_E and, in a the second one, I_E is related to the instrumental magnitude
86 M_i, the combined magnitude M_c (obtained, according to Rovida et al. (2020), as the merging or

87 the averaging of macroseismic and instrumental magnitudes), the epicentral intensity I_0 and the
88 maximum intensity I_{max}. The advantage of using such two-steps procedure is that for the first
89 step also the data of the pre instrumental era can be included in the analysis, whereas they must
90 be excluded if the calibration of the attenuation model is done simultaneously with instrumental
91 magnitude (available only since the beginning of 20th century).
92 The equation fitted by Pasolini et al. (2008b) in the first step is a log-linear function of the
93 hypocentral distance D

$$I = I_E - a(D - h) - b[\ln(D) - \ln(h)] \quad (1)$$

$$D = \sqrt{R^2 + h^2}$$

94 where a and b are empirical coefficients, R is the epicentral distance and h is an average focal
95 depth that is assumed to be the same for all the earthquakes and is empirically estimated
96 together with the other two coefficients. Owing to the logarithmic relationship mentioned
97 above between intensity and ground motion amplitude, the linear term of eq. (1) describes the
98 inelastic attenuation while the logarithmic term the geometrical spreading of seismic waves.
99 I_E can be calculated for each earthquake for which N intensity data I_i at hypocentral distances
100 D_i are available as

$$I_E = \bar{I} - a\bar{D} - b\overline{\ln(D)} \quad (2)$$

101 where

$$\bar{I} = \frac{1}{N}\sum_{I=1}^{N} I_i$$

$$\bar{D} = \frac{1}{N}\sum_{I=1}^{N} D_i \quad (3)$$

$$\overline{\ln(D)} = \frac{1}{N}\sum_{I=1}^{N} \ln(D_i)$$

102 Pasolini et al. (2008b) fitted such equation by maximizing the likelihood function obtained as
103 the product of the Normal probability densities of all intensity observations. In doing that, they

104 consider uncertain intensities, indicated in macroseismic practice by two adjacent degrees (e.g.
105 VII-VIII), as observations of both degrees, each taken with half weight. We will show that the
106 results of such procedure do not differ much from the ordinary least square (OLS) regression
107 method applied after converting uncertain intensities to real numbers (7.5 for VII-VIII).
108 Both regression methods attribute all the regression variance to the experimental error of the
109 intensity *I* only. This is correct because the uncertainty of the independent variable *D* can be
110 considered negligible with respect to the uncertainty of the dependent variable *I*. Conversely,
111 for the second step, the uncertainties of the independent variables M_i, M_c, I_0 and I_{max} are of the
112 same order magnitude of the uncertainty of the dependent variable I_E and then cannot be
113 neglected. Therefore, Pasolini et al. (2008b), fitted the linear equations of I_E with M_i, M_c, I_0 and
114 I_{max} using an error-in-variable (EIV) regression method (Fuller, 1987, Castellaro et al., 2006).
115 In our recalibration using the new DBMI15 V2.0 dataset, we will follow the same approach
116 but using the Chi-Square regression method (Stromeyer et al., 2004) that Lolli and Gasperini
117 (2012) showed to be equivalent to the EIV method of Fuller (1987) when the variances of the
118 two variables are constant, but which has the advantage of allowing the use of individual
119 variances for each observation when available.
120 Furthermore, also inspired by Mak et al. (2015), which observed a poor performance of the
121 IPE by Pasolini et al. (2008b) as a function of I_0, we will consider a different approach to
122 estimate the uncertainty of I_E to be used in EIV regressions. Pasolini et al (2008b) computed it
123 as the square root of "the average of the empirical variances computed for each earthquake in
124 the data set", so obtaining $\sigma(I_E)$=0.15 intensity degrees. We here estimate the uncertainty of I_E
125 from the empirical variance σ_E^2 of the linear regression of I_E with respect to $\underline{M_i}$

$$\sigma_E^2 = \frac{\sum_{j=1,N}\left(M_{i_j} - a - bI_{E_j}\right)^2}{N-2} \tag{4}$$

where a and b are respectively the intercept and the slope of the linear regression and N the number of data used.

As M_i and I_E are based on completely different information (instrumental and macroseismic data respectively), their uncertainties are totally independent to each other. Then a theoretical a-priori regression variance σ_T^2 can be computed as the combination of the variances of M_i and I_E by the error propagation law (see e. g. Stromeyer et al., 2004)

$$\sigma_T^2 = \frac{\sum_{j=1,N}\left[b^2\sigma^2\left(M_{i_j}\right) + \sigma^2\left(I_{E_j}\right)\right]}{N} \tag{5}$$

where $\sigma^2\left(M_{i_j}\right)$ and $\sigma^2\left(I_{E_j}\right)$ are the variances (the squares of uncertainties) of the j-th observations of M_i and I_E respectively. If the variance of I_E is assumed to be the same for all earthquakes, the previous equation becomes

$$\sigma_T^2 = b^2\frac{\sum_{j=1,N}\sigma^2\left(M_{i_j}\right)}{N} + \sigma^2(I_E) \tag{6}$$

from which we can get

$$\sigma^2(I_E) = \sigma_T^2 - \frac{b^2\sum_{j=1,N}\sigma^2\left(M_{i_j}\right)}{N} \tag{7}$$

The variances of magnitudes $\sigma^2\left(M_{i_j}\right)$ can be computed as the squares of magnitude uncertainties reported for each earthquake in the Catalogo Parametrico dei Terremoti Italiani (CPTI15) V2.0 catalog (Rovida et al., 2019, 2020).

Starting from an initial approximation of $\sigma^2(I_E)$, we can compute a preliminary regression from which to compute $\sigma^2(I_E)$ from eq. (7). Using such value, we recompute the regression up to obtain $\sigma_T^2 \cong \sigma_E^2$. This usually requires a few iterations because changing the variances of the regression variables implies a change of the coefficient b to be used in eq. (7).

The so determined variance $\sigma^2(I_E)$ can even be used for the EIV regressions of I_E with M_c, I_0 and I_{max}. In these cases, however the uncertainties of the regressed variables are somehow

correlated because I_0, I_{max} and, at least in part, even M_c are determined based on the intensity dataset used to determine I_E. Hence the empirical variances σ_E^2 of such regressions are expected to be lower than the theoretical ones σ_T^2.

For I_0 and I_{max}, we can argue that their variances should not differ much from that of I_E and then we can confidently assume equal variances in EIV regressions of I_E with respect to I_0 and I_{max}.

The dataset

The DBMI15 V2.0 dataset (Locati et al., 2019) collects in all 123,756 MDPs but a significant portion of them is not suitable to be used for fitting the IPE. In particular, 271 MDPs correspond to large areas without the indication of a precise location, 241 to individual buildings and 625 to small settlements that are unsuitable to provide a reliable intensity estimate. Of the remaining 122,619 MDPs, 5,960 are not real intensity estimates but only generic descriptions of effects (felt, damage, high damage, etc.) and 20,825 correspond to negative evidence (not felt).

According to Pasolini et al. (2008b), we discard all MDPs of degree II (3,531) because they correspond to a so weak feeling of ground shaking that might remain unobserved in most cases, and it is also difficult to be distinguished from degree III. We also discard the MDPs of earthquakes: a) with epicenter in the sea or close to the shore whose macroseismic epicentral location cannot be determined with reasonable accuracy (5,101), b) occurred before year 1200 A.D. (65), because they are based on scarcely reliable information, c) having less than 10 MDPs (5,431) because the macroseismic epicentral location might be inaccurate, d) occurred close to the summit of Mt. Etna (within 25 km from latitude 37.73 and longitude 15.00) and in other Italian volcanic regions (e.g. Ischia island and Flegrean Fields) (4,456), because the attenuation properties of such areas are known to be peculiar (highly attenuating) (Azzaro et al., 2006). In

order to prevent a bias due to the incompleteness of low intensities at large distances (Pasolini et al., 2008a), we also discard all MDPs (44,212) located at epicentral distances where an average intensity lower than IV is expected, based on a preliminary attenuation function. At end of the selection, 33,038 MDPs remain available for the fitting of the IPE (about 50% more than those used by Pasolini et al., 2008b).

In order to allow a comparison of our analysis with other IPEs which fits simultaneously distance and magnitude, we also compute the regressions for a reduced dataset of earthquakes for which the instrumental magnitude M_i is known. Such dataset includes in all 20,029 MDPs. Recently, Vannucci et al. (2021) showed that intensity estimates made in macroseismic surveys of Italian earthquakes occurred after year 2009 are not consistent with those made previously, possibly because they mostly adopted the EMS scale which was shown by Graziani et al. (2015) to underestimate the MCS scale of about 0.59±0.05 degrees on average in old town centers struck by the 2012 Emilia earthquakes where the building types were similar to those existing at the time when Sieberg (2012, 2032) formulated the MCS scale. Hence in the following, we will also consider for comparison a further reduced dataset limited to year 2009 (32,607 data).

For performing the second step of the procedure, we relate the intensity expected at the epicenter I_E, with the instrumental magnitude M_i, the combined magnitudes M_c, the epicentral intensity I_0 and the maximum intensity I_{max} as reported by the CPTI15 V2.0 catalog (labeled as M_{wins}, M_{wDef}, I_0 and I_{max} respectively).

As Vannucci et al. (2021) also found that instrumental magnitudes of Italian earthquakes occurred before 1960, mainly surface magnitudes Ms reported by Margottini et al. (1993), are likely to be overestimated owing to the poor dynamic calibration of mechanical recording seismometers (Herak 1996, 1998) operating in Italy and surrounding regions up to the

194 introduction of electromagnetic seismometers at the beginning of 1960's, we will also consider
195 the case of excluding such instrumental magnitudes from our second step computations.
196
197 **Isotropic attenuation results**
198
199 The results of the first step using the DBMI15 V2.0 dataset (Fig. 1 and Table 1) are very similar
200 (differences lower than 0.1 degree) to those obtained by Pasolini et al (2008b) using the
201 DBMI04 dataset (Stucchi et al., 2007). In the same Figure and Table, we also show the
202 comparison with other attenuation equations. In agreement with Pasolini et al. (2008b) the log-
203 linear (LOGLIN) model is statistically preferable, based on BIC (Schwarz, 1978) and AIC_c
204 (Akaike, 1974, Hurvich and Tsai, 1989) information criteria, with respect to all other models
205 excepting the log-bilinear one (LOGBIL) (see Pasolini et al., 2008b for details on various
206 models and on BIC and AICc information criteria). However, the improvement of the LOGBIL
207 model with respect to the LOGLIN one is relatively small so that to not deserve its adoption as
208 reference attenuation model, even considering the complications that this peculiar model would
209 introduce.
210 In Table 1 we also report the results of the regression of the log-linear model obtained by
211 excluding the intensity data of earthquakes occurred after year 2009 (LOGLIN (no >2009)),
212 which Vannucci et al. (2021) showed being significantly underestimated with respect to
213 previous periods. The regression standard deviation σ is slightly lower and the R^2 is slightly
214 higher, indicating a generally better fit with respect to that obtained using the entire dataset,
215 but the coefficients are not very different and thus such reduced dataset does not deserve further
216 consideration.
217 In Table 1 we also report the coefficients for the entire dataset obtained using the simple least
218 square method and considering uncertain intensities as real numbers (LOGLIN (LSQ)). The

219 differences with respect to the coefficients obtained by the procedure described by Pasolini et
220 al (2008b) are relatively small. In this case the various goodness of fit estimators (σ, R^2, AICc
221 and BIC) are not directly comparable with those obtained by the Pasolini et al. (2008b)
222 approach because the fitting methods are different.
223 The differences are larger with respect to the dataset considering only earthquakes for which
224 instrumental magnitude is provided (LOGLIN ($M_i \neq 0$)). In particular, the coefficient of the
225 linear term (describing the anelastic attenuation) is definitely smaller and the coefficient of the
226 logarithmic term (describing the geometrical spreading) definitely larger than for the whole
227 dataset. The reasons of such differences are not easy to explain and might refer to changes in
228 the way the intensities are estimated for earthquakes occurred before and after the beginning
229 of 1900. We might note that the former ones are mainly inferred from the scrutiny of written
230 documentary sources while the latter ones from on-site surveys or questionnaires.
231 In Fig. 2 and Table 2 we show the result of the second step regression between expected
232 intensity at the epicenter I_E and instrumental magnitude M_i. The uncertainty of I_E that makes
233 the theoretical regression standard deviation σ_T to coincide with the empirical one σ_E is
234 $\sigma(I_E)$=0.56 intensity degrees, more than three times larger than that assumed by Pasolini et al.
235 (2008b) and of the same order of magnitude of the uncertainties attributed by them to the
236 uncertainties of epicentral intensity I_0 and maximum intensity I_{max} (0.5 degrees).
237 We use such value of $\sigma(I_E)$ even for the regression with combined magnitude M_c shown in
238 Fig. 3. As expected, in the latter case the empirical standard deviation σ_E is smaller than the
239 theoretical one σ_T because the two regressed variables are both based, at least in part, on the
240 same intensity data.
241 The coefficients of the two regressions are rather different from those computed by Pasolini et
242 al. (2008b). In fact, the larger value of the variance we adopted here for I_E has the effect of
243 reducing the slope coefficient (e.g., Castellaro and Bormann, 2007). According to Pasolini, et

al. (2008b), for computing I_E from magnitudes, we suggest using the coefficients of the regression with M_c because it is based on a larger number of earthquakes, which actually correspond to those used in Italian seismic hazard analyses.

In Fig. 4 and 5 and in Table 2 we show the results of the regressions of I_E with I_0 and I_{max} respectively. We can note that, differently from Pasolini et al. (2008b), the slopes b are now very close to 1. The Student's t-test indicates in both cases that the H_0 hypothesis (b=1) cannot confidently rejected with significance levels (s.l.) p=0.69 and p=0.41 respectively. This means that to compute I_E from I_0 and I_{max} it is sufficient to apply constant shifts rather than the linear regression formulas. For I_0, even the H_0 hypothesis that the shift Δ=0 cannot be confidently rejected (with p=0.15) and then it can be simply assumed that I_E coincides with I_0, whereas for I_{max}, the required shift Δ=-0.22±0.03 is significantly different from 0 and then must be applied to compute I_E from $I_{max.}$

In Table 2 bottom and in Figures S1 to S4 of the supplemental material we report the results of regressions between I_E and M_i, M_c, I_0 and I_{max} for the dataset considering only earthquakes for which instrumental magnitude is provided (LOGLIN ($M_i \neq 0$)). The coefficients in this case are not very different from those of the full dataset. In table S1 of the supplemental material we also report the coefficients of various intensity attenuation laws for the same dataset, whereas in table S2 we report the results of regressions between I_E and M_i, M_c, I_0 and I_{max} for a dataset excluding MDPs of earthquakes occurred after year 2009 and with $M_i \neq 0$ only in years ≥1960. Even in such cases the differences with respect to the full set are relatively small.

In summary the new equations (based on the full set of intensity data) we suggest using are

$$I = I_E - (0.0081 \pm 0.0004)(D - h) - (1.072 \pm 0.024)[\ln(D) - \ln(h)] \qquad (8)$$

where h = (4.49±0.22) km.

If MDPs are available for the earthquake, I_E can be computed by eqs. (2) and (3), otherwise by

$$I_E = -(2.578 \pm 0.145) + (1.867 \pm 0.028)M_w \quad (9)$$

$$I_E = I_0$$

For the dataset limited to earthquakes (since year 1904) for which an instrumental magnitude is available, the equations are (see Table 1 and 2):

$$I = I_E - (0.0066 \pm 0.0005)(D - h) - (1.235 \pm 0.034)[\ln(D) - \ln(h)] \quad (10)$$

Where h = (6.35±0.34) km.

In the absence of MDPs, I_E can be computed as

$$I_E = -(1.459 \pm 0.251) + (1.610 \pm 0.051)M_w \quad (11)$$

$$I_E = -(0.08 \pm 0.01) + I_0$$

In Fig. 6 (and Table S5 and S6 in the supplemental material) we report the mean intensity residuals (observed-computed) as a function of hypocentral distance (a) and computed (predicted) intensity (b). They are very small (of the order of 0.1 degrees or less), in many cases within (1σ) error bounds, and do not show particular trends.

Tomographic inversion results

This analysis has to be considered preliminary and is shown here only to give a picture of possible attenuation heterogeneities in the Italian territory.

We approached the problem similarly to Carletti and Gasperini (2003) but using the log-linear attenuation model in place of the bilinear one used by them. We keep fixed the b coefficient (representing the geometrical spreading) and the average depth h to the values determined in the isotropic case and let to vary the a coefficient (representing inelastic attenuation) on 252 spatial cells with sides of about 32 km covering the entire Italian area. We take as reference the coefficients computed by the standard LSQ approach using uncertain intensities as semi-integer (b=1.075 and h=4.61) because even for the tomographic inversion we had to adopt the

288 same fitting strategy. The goodness of fit parameters indicated in Table 1 for the tomographic
289 inversion are thus comparable with that of the OLS inversion and, as expected, show a lower
290 σ and a higher R^2 for the tomographic model. The result of information criteria BIC and AICc,
291 which penalize more the tomographic model having a larger number of free parameters (256)
292 than the isotropic one (4), are contradictory as for BIC the most preferable model is the
293 isotropic one whereas for AICc it is the tomographic one.
294 In Fig. 7 we show the plot of the differences of the *a* coefficient computed in each cell for the
295 tomographic model with respect to the isotropic (LSQ) value (0.0079). Positive residuals (blue)
296 indicate lower attenuation and negative ones (red) higher attenuation than the average isotropic
297 model. In Fig. 8 we show the epicenter-to-locality paths showing a good coverage in all
298 continental Italy excepting for extreme northwestern and southeastern areas.
299 Like Carletti and Gasperini (2003), we find low attenuation (blue) in the Po plain where a
300 homogeneous carbonatic bedrock well propagate seismic waves and high attenuation (red) in
301 the south-western slope of the Apennines where the bedrock is highly fractured and high heat
302 flow (Della Vedova et al., 1991), related to primary and secondary volcanic activities, produces
303 relatively high temperatures in the Earth's crust.
304

305 **Conclusions**

306

307 We have recomputed the coefficients of a log-linear intensity prediction equation in Italy,
308 following the procedure by Pasolini et al. (2008b). We used the intensity data of the DBMI15
309 V2.0 (Locati et al., 2019) intensity database and the instrumental and combined (instrumental
310 plus macroseismic) magnitudes and the epicentral and maximum intensities reported by the
311 CPTI15 V2.0 catalog. The coefficients of the linear and logarithmic terms (eq. 8) are not very
312 different from those obtained by Pasolini et al. (2008b) using the DBMI04 dataset (Stucchi et

al., 2007). We obtained instead different coefficients of regressions of the expected intensity at the epicenter with respect to the magnitudes and the epicentral and maximum intensities (eq. 9) because we modified the approach to estimate the uncertainties used error-in-variable regression methods. The latter are necessary because the uncertainties of the independent variables are not negligible with respect to those of the dependent one.

We also made a preliminary tomographic inversion of the lateral variations of the coefficient of the linear term representing the inelastic attenuation that confirm previous analyses: low attenuation in the Po valley where a homogeneous carbonatic bedrock (e.g. Fantoni and Franciosi, 2010) well propagate seismic waves and high attenuation in the Thyrrenian slope of the Apennines where high heat flow (Della Vedova et al., 1991) related to volcanic activity induce a degradation of the rock quality factor.

Acknowledgements

We thank the associate editor and three reviewers for useful comments and suggestions.

Data and resource section

The "Database Macrosismico Italiano (DBMI15), V2.0" is downloaded from https://emidius.mi.ingv.it/CPTI15-DBMI15_v2.0/ (last accessed July 5th 2023). The "

The "Catalogo Parametrico dei Terremoti Italiani (CPTI15), V2.0" is downloaded from https://emidius.mi.ingv.it/CPTI15-DBMI15_v2.0/ (last accessed July 5th 2023).

Conflict of interest: The authors declare that there is no conflict of interest regarding the publication of this manuscript.

338

339 **References**

340

341 Akaike, H. (1974), A new look at the statistical model identification, IEEE Trans. Autom.
342 Control, AC-19, 716 – 723, doi:10.1109/TAC.1974.1100705.

343

344 Albarello, D., F. Bramerini, V. D'Amico, A. Lucantoni, and G. Naso (2002). Italian intensity
345 hazard maps: a comparison of results from different methodologies, Boll. Geofis. Teorica Appl.
346 43, 249–262.

347

348 Atkinson, G. M., and S. I. Kaka (2007). Relationships between felt intensity and instrumental
349 ground motion in the central United States and California, Bull. Seismol. Soc. Am. 97, 497–
350 510, doi: 10.1785/0120060154.

351

352 Azzaro, R., Barbano, M. S., D'Amico, S. and Tuvè, T. (2006). The attenuation of seismic
353 intensity in the Etna region and comparison with other Italian volcanic districts, Ann.
354 Geophys., 49, 1003-1020.

355

356 Cancani, A. (1904). Sur l'emploi d'une double echelle sismique des intensités, empirique et
357 absolute, G. Beitr., Erganzungsband 2, 281-283 (in French).

358

359 Carletti F. and Gasperini P. (2003). Lateral variations of seismic intensity attenuation in Italy,
360 Geophys. J. Int., 155, 839-856, doi: 10.1111/j.1365-246X.2003.02073.x.

361

362 Castellaro, S., Mulargia, F. & Kagan, Y.Y. (2006). Regression problems for magnitudes,
363 Geophys. J. Int., 165, 913–930. Doi: 10.1111/j.1365-246X.2006.02955.x

364

365 Castellaro, S. & Bormann, P. (2007). Performance of Different Regression Procedures on the
366 Magnitude Conversion Problem, Bull. Seism. Soc. Am., 97/4, 1167-1175. doi:
367 10.1785/0120060102.

368

369 Cornell, C. A. (1968). Engineering seismic risk analysis, Bull. Seism. Soc. Am. 58, 1583–1606,
370 doi: 10.1785/BSSA0580051583.

371

372 Della Vedova, B., Mongelli, F., Pellis, G., Squarci, P., Taffi, L. & Zito, G., 1991. Heat flow
373 map of Italy, International Institute for Geothermal Research, CNR-Pisa.

374

375 Faenza L, Michelini A (2010) Regression analysis of MCS intensity and ground motion
376 parameters in Italy and its application in ShakeMap. Geophys J Int 180:1138–1152. doi:
377 10.1111/ j.1365-246X.2009.04467.x.

378

379 Fantoni, R. and Franciosi, R. (2010) Tectono-sedimentary Setting of the Po Plain and Adriatic
380 Foreland. Rendiconti Lincei - Scienze Fisiche e Naturali, 21, S197-S209, doi: 10.1007/s12210-
381 010-0102-4.

382

383 Fuller, W.A. (1987). Measurement Error Models, John Wiley, pp. 440.

384

385 Gasperini P., Bernardini F., Valensise G. and Boschi E. (1999). Defining seismogenic sources
386 from historical felt reports, Bull. Seism Soc. Am., 89, 94-110, doi: 10.1785/BSSA0890010094.

387

388 Gasperini P., Vannucci G., Tripone D. and Boschi E. (2010). The Location and Sizing of
389 Historical Earthquakes Using the Attenuation of Macroseismic Intensity with Distance, Bull.
390 Seismol. Soc. Am., 100, 2035–2066, doi: 10.1785/0120090330.
391
392 Gasperini P., Lolli B. and Vannucci G. (2013). Empirical Calibration of Local Magnitude Data
393 Sets Versus Moment Magnitude in Italy, Bull., Seism. Soc. Am., 103, 2227-2246, doi:
394 10.1785/0120120356.
395
396 Gómez Capera, A. A., D'Amico V., Meletti. C., Rovida A. and Albarello D. (2010). Seismic
397 Hazard Assessment in Terms of Macroseismic Intensity in Italy: A Critical Analysis from the
398 Comparison of Different Computational Procedures, Bull., Seism. Soc. Am., 100/4, 1614-
399 1631, doi: 10.1785/0120090212.
400
401 Gomez-Capera, A. A., D'Amico, M., Lanzano, G., Locati, M., and Santulin, M. (2020).
402 Relationships between ground motion parameters and macroseismic intensity for Italy, Bull.
403 Earth. Eng. 18, 5143-5164, doi: 10.1007/s10518-020-00905-0.
404
405 Graziani, L., F. Bernardini, C. Castellano, S. Del Mese, E. Ercolani, A. Rossi, A. Tertulliani,
406 and M. Vecchi (2015). The 2012 Emilia (Northern Italy) earthquake sequence: An attempt of
407 historical reading, J. Seismol. 19, 371–387, doi: 10.1007/s10950-014-9471-y.
408
409 Grünthal, G. (ed.) (1998). European macroseismic scale 1998, *Conseil de l'Europe. Cahiers*
410 *du Centre Européen de Géodynamique et de Séismologie,*13, Luxembourg, 99 pp.
411

412 Herak, M., I. Allegretti, D. Herak, and S. J. Duda (1996). Calibration of the Wiechert
413 seismographs relative to a reference seismometer, Geofizika 13, 31–59.
414
415 Herak, M., I. Allegretti, D. Herak, and S. J. Duda (1998). Numerical modeling of the observed
416 Wiechert seismograph magnification, Pure Appl. Geophys. 152, 539–550.
417
418 Hurvich, C. M., and C.-L. Tsai (1989), Regression and time series model selection in small
419 samples, Biometrika, 76, 297–307, doi:10.1093/biomet/76.2.297.
420
421 Locati M., Camassi R., Rovida A., Ercolani E., Bernardini F., Castelli V., Caracciolo C.H.,
422 Tertulliani A., Rossi A., Azzaro R., D'Amico S., Conte S., Rocchetti E., Antonucci A. (2019).
423 Database Macrosismico Italiano (DBMI15), versione 2.0. Istituto Nazionale di Geofisica e
424 Vulcanologia (INGV), doi: 10.13127/DBMI/DBMI15.2.
425
426 Locati M., Camassi R., Rovida A., Ercolani E., Bernardini F., Castelli V., Caracciolo C.H.,
427 Tertulliani A., Rossi A., Azzaro R., D'Amico S., Antonucci A. (2021). Database Macrosismico
428 Italiano (DBMI15), versione 3.0. Istituto Nazionale di Geofisica e Vulcanologia (INGV), doi:
429 10.13127/DBMI/DBMI15.3.
430
431 Locati M., Camassi R., Rovida A., Ercolani E., Bernardini F., Castelli V., Caracciolo C.H.,
432 Tertulliani A., Rossi A., Azzaro R., D'Amico S., Antonucci A. (2022). Database Macrosismico
433 Italiano (DBMI15), versione 4.0. Istituto Nazionale di Geofisica e Vulcanologia (INGV), doi:
434 10.13127/DBMI/DBMI15.4
435

436 Lolli B., Gasperini P. (2012). A comparison among general orthogonal regression methods
437 applied to earthquake magnitude conversions, Geophys. J. Int., 190, 1135-1151, doi:
438 10.1111/j.1365-246X.2012.05530.x.
439
440 Lolli B., Gasperini P. and Vannucci G. (2014). Empirical conversion between teleseismic
441 magnitudes (mb andMs) and moment magnitude (Mw) at the Global, Euro-Mediterranean and
442 Italian scale, Geophys. J. Int., 199, 805–828, doi: 10.1093/gji/ggu264.
443
444 Lolli, B., C. Pasolini, P. Gasperini, and G. Vannucci (2019). Prodotto 4.8: Ricalibrazione
445 dell'equazione di previsione di Pasolini et al. (2008), in Il modello di pericolosità sismica
446 MPS19. Rapporto finale, Centro Pericolosità Sismica, C. Meletti and W. Marzocchi (Editors),
447 Istituto Nazionale di Geofisica e Vulcanologia, maggio 2019, Roma, 168 pp (in Italian).
448
449 Mak S., Clemens R. A. and Schorlemmer D. (2015). Validating Intensity Prediction Equations
450 for Italy by Observations, Bull. Seism Soc. Am., 105, 2942–2954, doi: 10.1785/0120150070.
451
452 Margottini, C., N. N. Ambraseys, and A. Screpanti (1993). La magnitudo dei terremoti italiani
453 del XX Secolo, E.N.E.A. Internal Publication, Rome, Italy, 57 pp. (in Italian).
454
455 McGuire, R. K. (Editor) (1993). The Practice of Earthquake Hazard Assessment, Int. Assoc.
456 Seism. Phys. Earth Interiors (IASPEI), Denver, Colorado, 284 pp.
457
458 Meletti, C., Marzocchi, W., D'amico, V., Lanzano, G., Luzi, L., Martinelli, F., Pace, B.,
459 Rovida, A., Taroni, M., Visini, F., Akinci, A., Anzidei, M., Avallone, A., Azzaro, R., Barani,
460 S., Barberi, G., Barreca, G., Basili, R., Bird, P., Bonini, M., Burrato, P., Busetti, M., Camassi,

461 R., Carafa, M.M.C., Cavaliere, A., Cecere, G., Cheloni, D., Chioccarelli, E., Console, R., Corti,
462 G., D'agostino, N., Cin, M.D., D'ambrosio, C., D'amico, M., D'amico, S., Devoti, R., Esposito,
463 A., Faenza, L., Falcone, G., Felicetta, C., Fracassi, U., Franco, L., Galvani, A., Gasperini, P.,
464 Gee, R., Gómez Capera, A.A.., Iervolino, I., Kastelic, V., Lai, C.G., Locati, M., Lolli, B.,
465 Maesano, F.E., Marchesini, A., Mariucci, M.T., Martelli, L., Massa, M., Metois, M., Monaco,
466 C., Montone, P., Moschetti, M., Murru, M., Pacor, F., Pagani, M., Pasolini, C., Peresan, A.,
467 Peruzza, L., Pietrantonio, G., Poli, M.E., Pondrelli, S., Puglia, R., Rebez, A., Riguzzi, F.,
468 Roselli, P., Rotondi, R., Russo, E., Sani, F., Santulin, M., Selvagg,i G., Scafidi, D., Selva, J.,
469 Sepe, V., Serpelloni, E., Slejko, D., Spallarossa, D., Stallone, A., Tamaro, A., Tarabusi, G.,
470 Tiberti, M.M., Tuvè, T., Valensise, G., Vallone, R., Vannoli, P., Vannucci, G., Varini, E.,
471 Zanferrari, A., Zuccolo, E., Danciu, L., Schorlemmer, D., Bazzurro, P., Giardini, D., Modena,
472 C., Mulargia, F., Seno, S. (2021). The new Italian seismic hazard model (MPS19), Ann. of
473 Geophys., 64/1, SE112. doi:10.4401/ag-8579.
474
475 Oliveti, I., Faenza, L. and Michelini, A. (2022). New reversible relationships between ground
476 motion parameters and macroseismic intensity for Italy and their application in ShakeMap,
477 Geophys. J. Int., 231, 1117-1137, doi: 10.1093/gji/ggac245.
478
479 Pasolini C., Gasperini P., Albarello D., Lolli B. and D'Amico V. (2008a). The attenuation of
480 seismic intensity in Italy part I: theoretical and empirical backgrounds, Bull. Seism. Soc. Am.,
481 98, 682–691, doi: 10.1785/0120070020.
482
483 Pasolini C., Albarello D., Gasperini P., D'Amico V. and Lolli B. (2008b). The attenuation of
484 seismic intensity in Italy part II: modeling and validation, Bull. Seism. Soc. Am., 98, 692–708,
485 doi: 10.1785/0120070021.

Rovida A., Locati M., Camassi R., Lolli B., Gasperini P. (2019). Catalogo Parametrico dei Terremoti Italiani (CPTI15), versione 2.0. Istituto Nazionale di Geofisica e Vulcanologia (INGV). https://doi.org/10.13127/CPTI/CPTI15.2

Rovida, A., M. Locati, R. Camassi, B. Lolli, and P. Gasperini (2020), The Italian earthquake catalogue CPTI15, Bull. Earth. Eng., 18, 2953-2984, doi: 10.1007/s10518-020-00818-y.

Schwarz, G. (1978), Estimating the dimension of a model, Ann. Stat., 6, 461– 464, doi:10.1214/aos/1176344136

Sieberg, A. (1912): Über die makroseismische Bestimmung der Erdbebenstärke. Ein Beitrag zur seismologische Praxis, G.Gerlands Beiträge zur Geophysik, 11 (2-4), 227-239 (in German).

Sieberg, A. (1932): Erdebeben, in Handbuch der Geophysik, Vol. 4, (B. Gutenberg Ed.), 552-554 (in German).

Stromeyer, D., Grünthal, G. & Wahlström, R., 2004. Chi-square regression for seismic strength parameter relations, and their uncertainties, with applications to an Mw based earthquake catalogue for central, northern and northwestern Europe, J. Seismol., 8(1), 143–153, doi: 10.1023/B:JOSE.0000009503.80673.51.

Stucchi , M., R. Camassi, A. Rovida, M. Locati, E. Ercolani, C. Meletti, P. Migliavacca , F. Bernardini and R. Azzaro (2007). DBMI04, il database delle osservazioni macrosismiche dei

510 terremoti italiani utilizzate per la compilazione del catalogo parametrico CPTI04. Quaderni di
511 Geofisica, Vol 49, pp.38, doi: 10.6092/INGV.IT-DBMI04 (in Italian).
512
513 Tselentis G, Danciu L (2008) Empirical relationships between modified Mercalli intensity and
514 engineer- ing ground-motion parameters in Greece. Bull Seismol Soc Am 98(4):1863–1875,
515 doi: 10.1785/0120070172.
516
517 Vannucci, G., B. Lolli, and P. Gasperini (2021). Inhomogeneity of Macroseismic Intensities in
518 Italy and Consequences for Macroseismic Magnitude Estimation, Seismol. Res. Lett. 92,
519 2234–2244, doi: 10.1785/0220200273.
520
521 Wald, DJ, Quitoriano V, Heaton TH, Kanamori H (1999) Relations between peak ground
522 acceleration, peak ground velocity, and modified Mercalli intensity in California. Earthq.
523 Spectra, 15(3):557–564, doi: 10.1193/1.1586058.
524
525 Zanini MA, Hofer L, Faleschini F (2019) Reversible ground motion-to-intensity conversion
526 equations based on the EMS-98 scale. Eng Struct 180:310–320, doi:
527 10.1016/j.engstruct.2018.11.032.
528

Figure 1

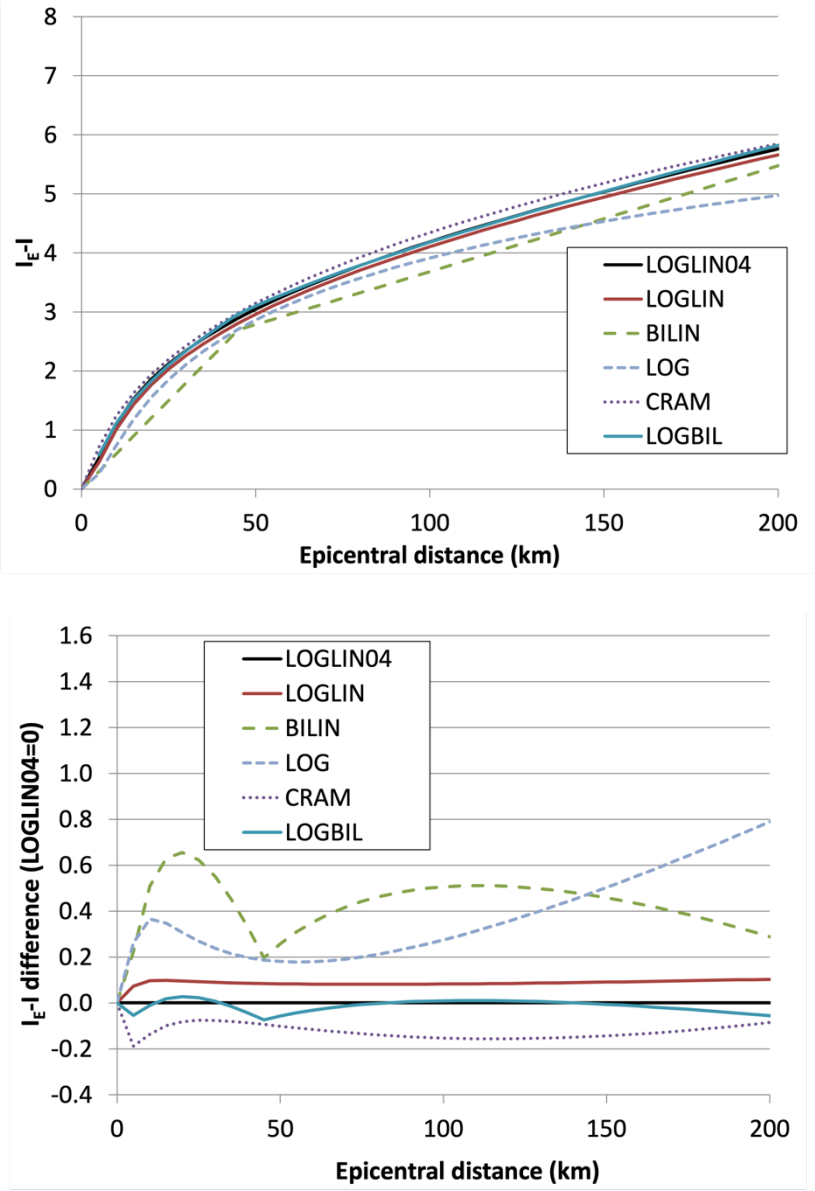

Figure 1 – Comparison between different attenuation laws. Top: differences betwen the expected intensity at the epicenter I_E and intensity at the site I for various attenuation functions (LOGLIN: Log linear, BILIN: bilinear, LOG: logarithmic, CRAM: cubic root, LOGBIL: logarithmic bilinear) as a function of epicentral distance R. Bottom differences of previous curves with respect to the loglinear model fitted on the DBMI04 dataset by Pasolini et al. (2008b) (LOGLIN04).

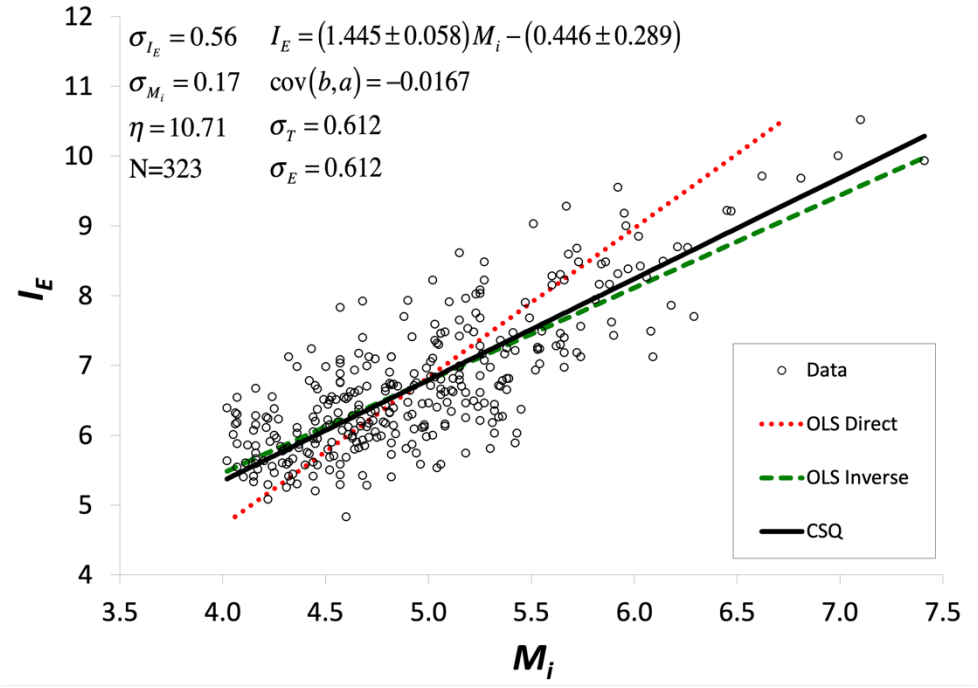

Figure 2 – Regression between I_E and M_i using the chisquare (CSQ) and ordinary least squares (OLS) methods. σ_{I_E} and σ_{M_i} are the uncertainties of I_E and M_i respectively, η their ratio, N the number of data, σ_T and σ_E respectively the theoretical and empirical regression standard deviations.

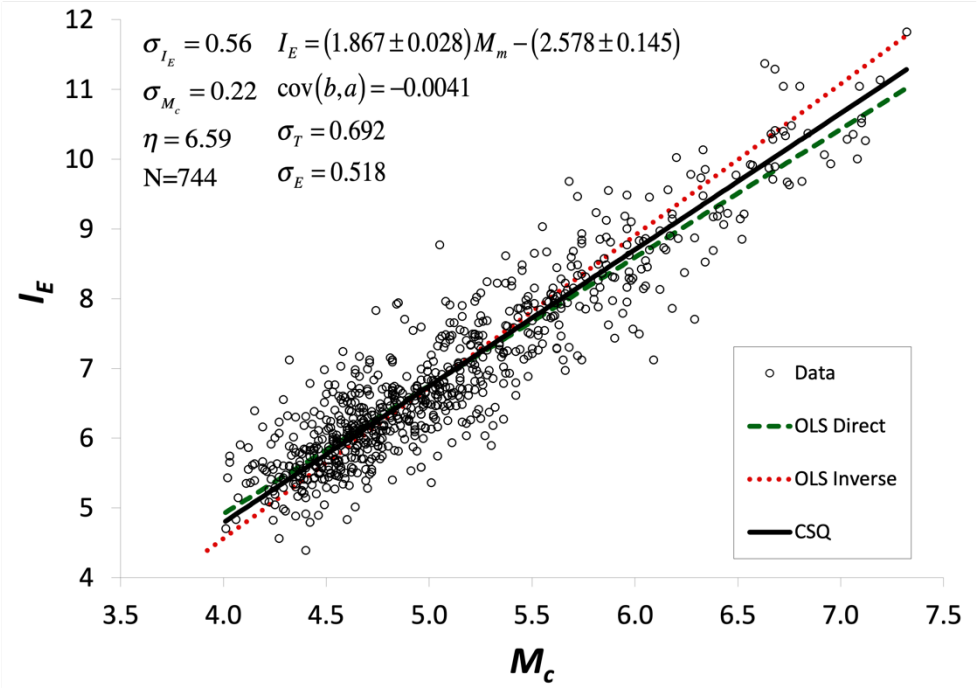

Figure 3 – As in Fig. 2 for regression between I_E and M_c.

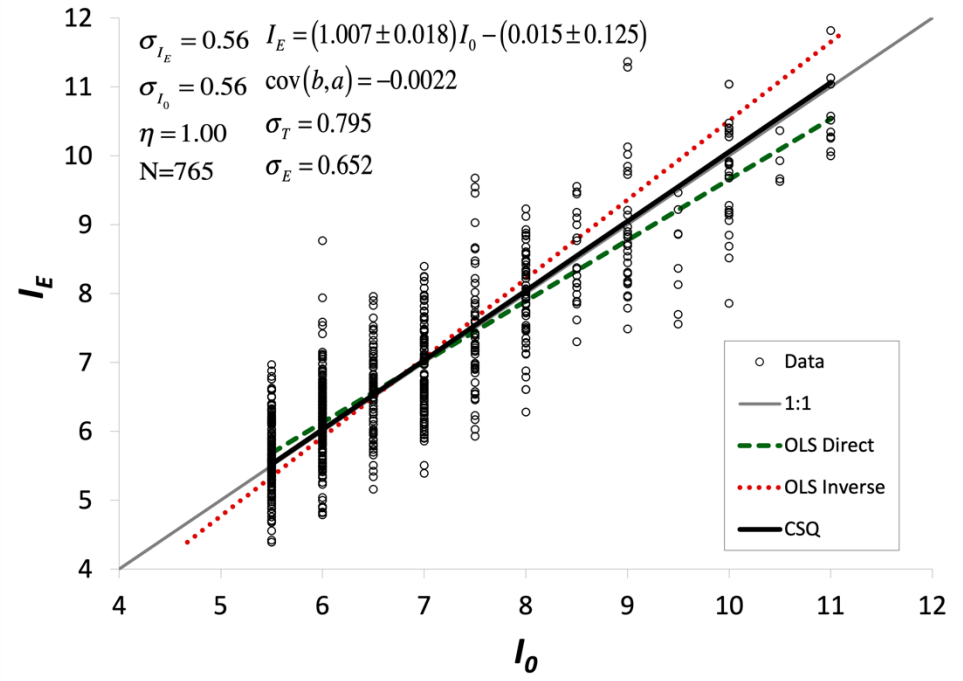

Figure 4 – As in Fig. 2 for regression between I_E and I_0.

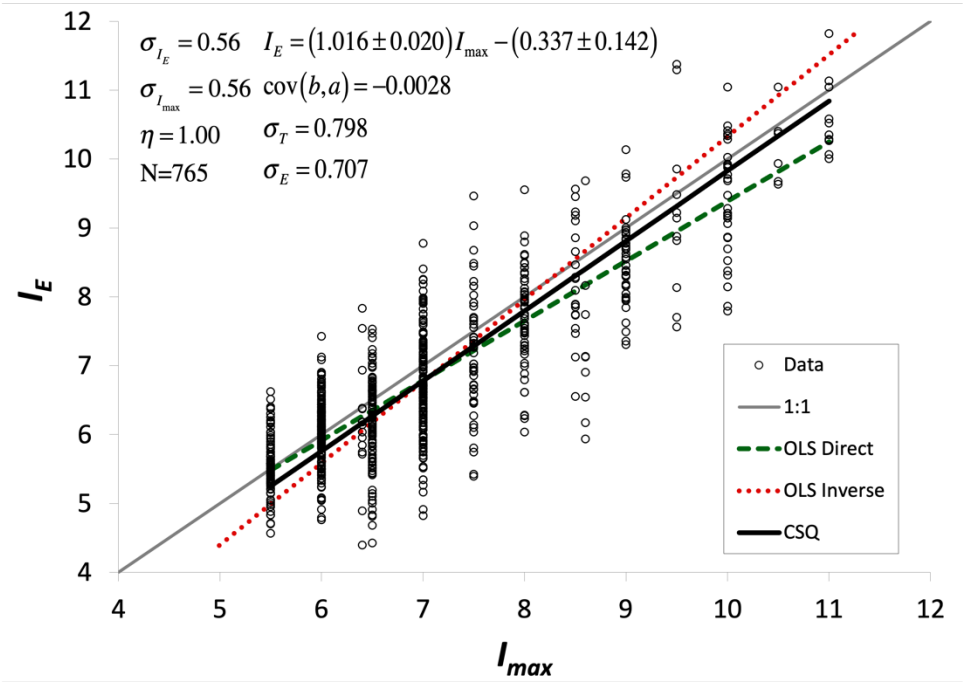

Figure 5 – As in Fig. 2 for regression between I_E and I_{max}.

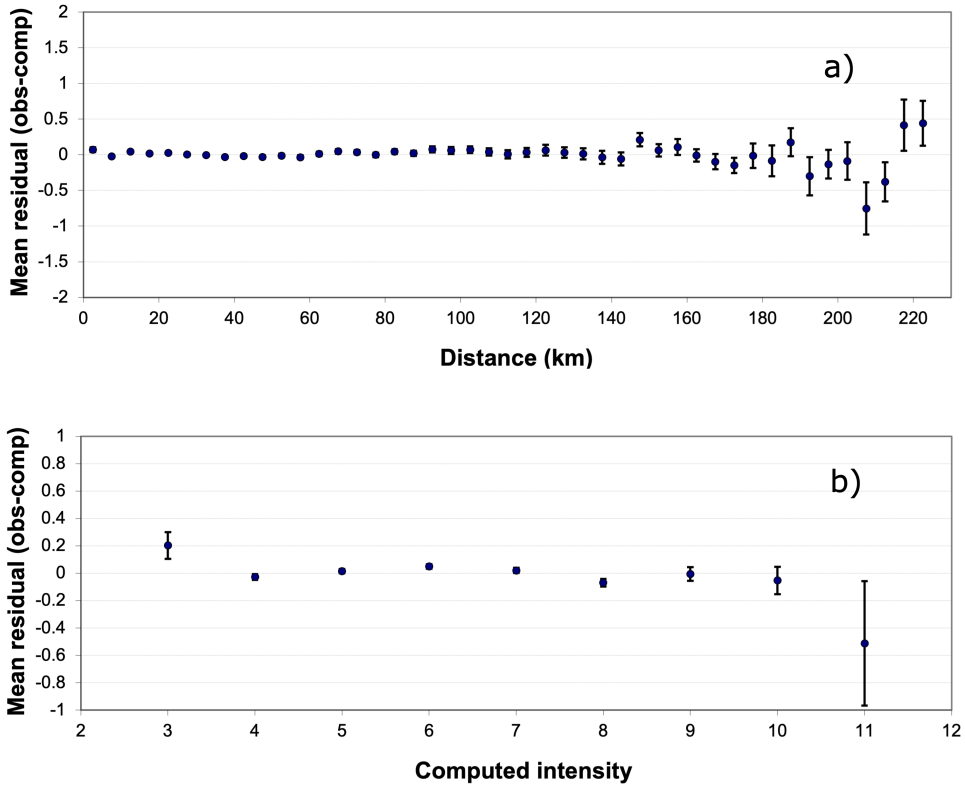

553

554 **Figure 6 – Mean intensity residuals (observed-computed) as a function of hypocentra**
555 **distance (a) and of computed intensity (b) for the preferred attenuation model (LOGLIN**
556 **in Table 1).**

557

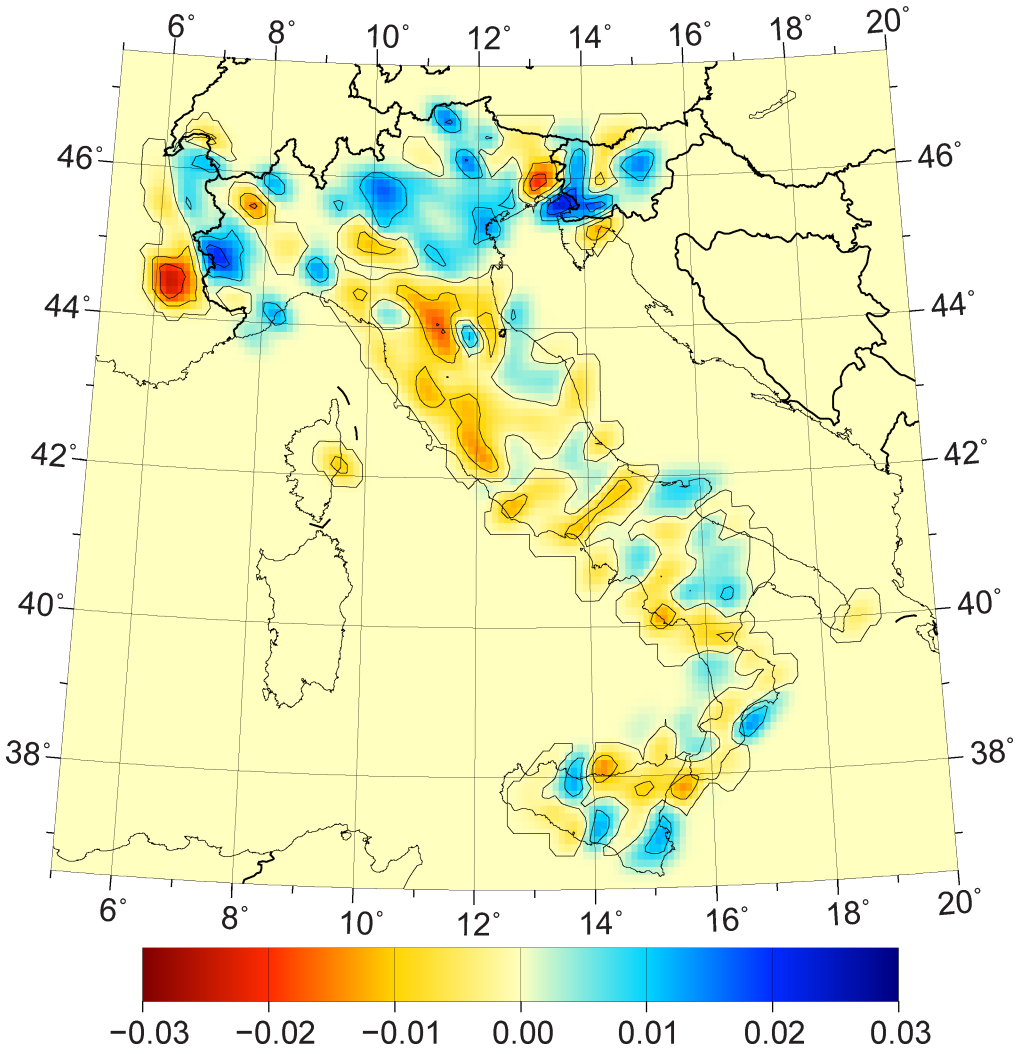

Figure 7 – Differences of the *a* coefficient of the LOGLIN (LSQ) attenuation law with respect to the value (-0.0079) computed for the isotropic model.

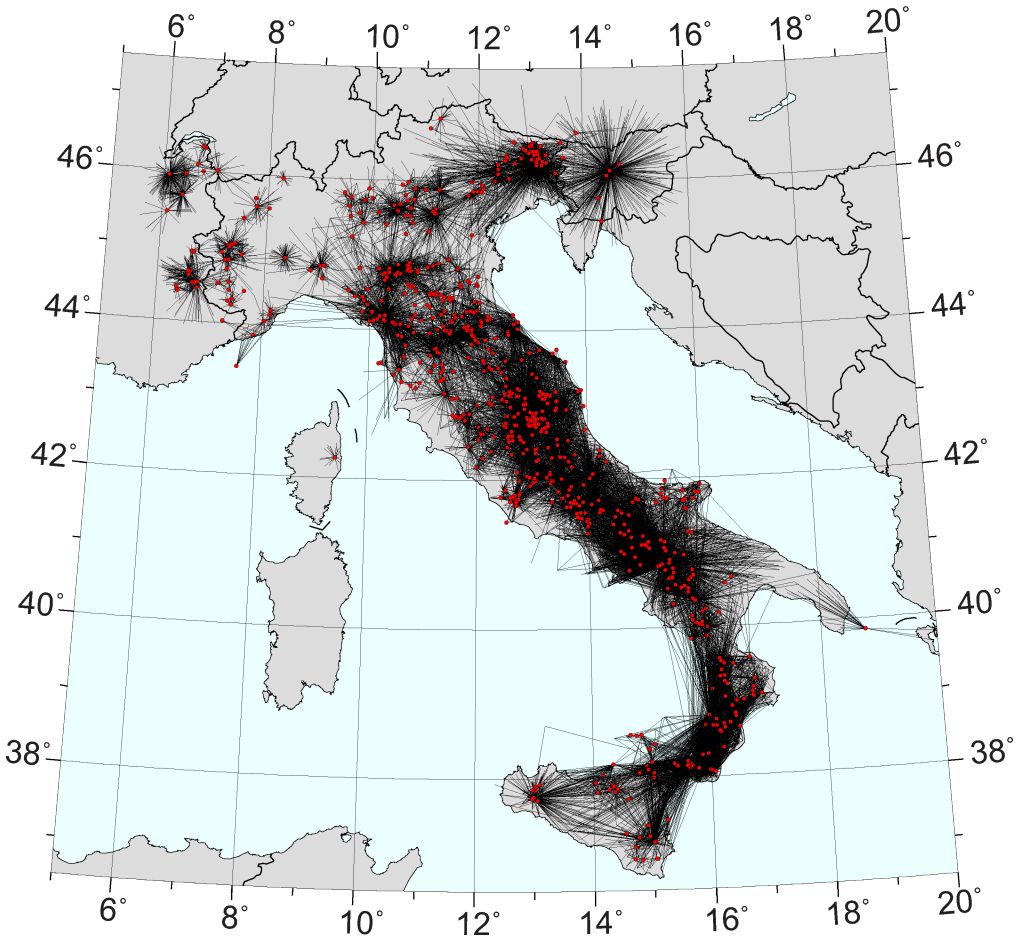

562

563 **Figure 8 – Epicenter-to-locality paths (in black) used for tomographic inversion of Fig. 7.**

564 **Red dots indicate the macroseismic epicenters of selected earthquakes.**

565

Table 1 – Regression coefficients for different attenuation models and datasets

Atten. Mod.	***N***	***a***	***a'***	***b***	***knee* (km)**	***h*(km)**	**σ**	**R^2**	**BIC**	**AICc**
LOGLIN 04[+]	4	*-0.0086±0.0005*	-	*-1.037±0.027*	-	*3.91±0.27*	*0.689360*	*0.656482*	-	-
LOGLIN	**4**	**-0.0081±0.0004**	**-**	**-1.072±0.024**	**-**	**4.49±0.22**	**0.652742**	**0.642909**	**-37352.6**	**-37344.5**
BILIN	4	-0.0599±0.0004	-0.0179±0.0002	-	45	0.00±0.19	0.664555	0.629866	-37812.6	-37804.5
LOG	3	-	-	-1.535±0.012	-	7.84±0.18	0.656656	0.638613	-37497.3	-37491.5
CRAM	3	-	-	-1.250±0.007	-	1.59±0.17	0.653061	0.642559	-37361.7	-37355.9
LOGBIL	5	-0.0217±0.0020	-0.0122±0.0005	-0.748±0.046	45	2.90±0.30	0.652375	0.643310	-37341.5	-37331.1
LOGLIN (no >2009)	4	-0.0084±0.0004	-	-1.062±0.023	-	4.43±0.22	0.650965	0.645965	-	-
LOGLIN ($M_i \neq 0$)	4	-0.0066±0.0005	-	-1.235±0.034	-	6.35±0.34	0.626567	0.671654	-	-
LOGLIN (LSQ)	4	-0.0079±0.0004	-	-1.075±0.023	-	4.61±0.22	0.739919	0.775855	-36965.6	-36926.9
LOGLIN (TOMO)	256	*	-	-1.075±0.023	-	4.61±0.22	0.720637	0.797755	-37159.1	-36509.4

In **bold type** the overall suggested/preferred coefficients. [+]From Pasolini et al. (2008a). *N* number of free parameters, *a* coefficient of the linear term (unique or before the knee for bilinear models), *a'* coefficient of the linear term after the knee (for bilinear models), *b* coefficient of logarithmic term for LOG, LOGLIN and LOGBIL models and of the cubic root for CRAM model, *h* source depth, σ regression standard deviation, R^2 regression coefficient of determination, BIC and AICc Bayesan and corrected Akaike information criteria (the higher the score the better the

model). “no >2009” indicates the dataset excluding intensity data of earthquakes after 2009, “$M_i \neq 0$” dataset with only earthquakes having instrumental magnitude., LSQ least square regression, TOMO spatially variable inversion for parameter *a*.

Table 2 – Linear regressions of expected intensity at the epicenter I_E with instrumental M_i and combined M_c magnitudes and epicentral I_0 and maximum I_{max} intensities

Regression	Dataset	N	a (intercept)	b (slope)	$p(b=1)$	σ	Δ	$p(\Delta=0)$
I_E-M_i	Full	323	-0.446±0.289	1.445±0.058	<0.01	0.61	-	-
I_E-M_c	Full	744	-2.578±0.145	1.867±0.028	<0.01	0.52	-	-
I_E-I_0	Full	765	-0.015±0.125	1.007±0.018	0.69	0.65	0.03±0.02	0.15
I_E-I_{max}	Full	765	-0.337±0.141	1.002±0.020	0.41	0.69	-0.22±0.03	<0.01
I_E-M_i	$M_i \neq 0$	323	-0.707±0.292	1.454±0.058	<0.01	0.62	-	-
I_E-M_c	$M_i \neq 0$	338	-1.459±0.251	1.610±0.051	<0.01	0.53	-	-
I_E-I_0	$M_i \neq 0$	356	0.078±0.193	0.974±0.029	0.22	0.60	-0.08±0.02	<0.01
I_E-I_{max}	$M_i \neq 0$	356	-0.176±0.220	0.981±0.032	0.38	0.66	-0.28±0.03	<0.01

N number of data, $p(b=1)$ probability of Student's t test of the H_0 hypothesis that $b=1$, σ regression standard deviation, Δ offset, $p(\Delta=0)$ probability of Student's t test of the H_0 hypothesis that $\Delta=0$. "$M_i \neq 0$" dataset with only earthquakes having instrumental magnitude.

Recalibration of the intensity prediction equation in Italy using the new Macroseismic Dataset DBMI15 V2.0

Lolli[1] B., Gasperini[2,1] P., Vannucci[2] G.

[1]Istituto Nazionale di Geofisica e Vulcanologia, Sezione di Bologna

[2]Dipartimento di Fisica e Astronomia, Università di Bologna

Supplemental Material

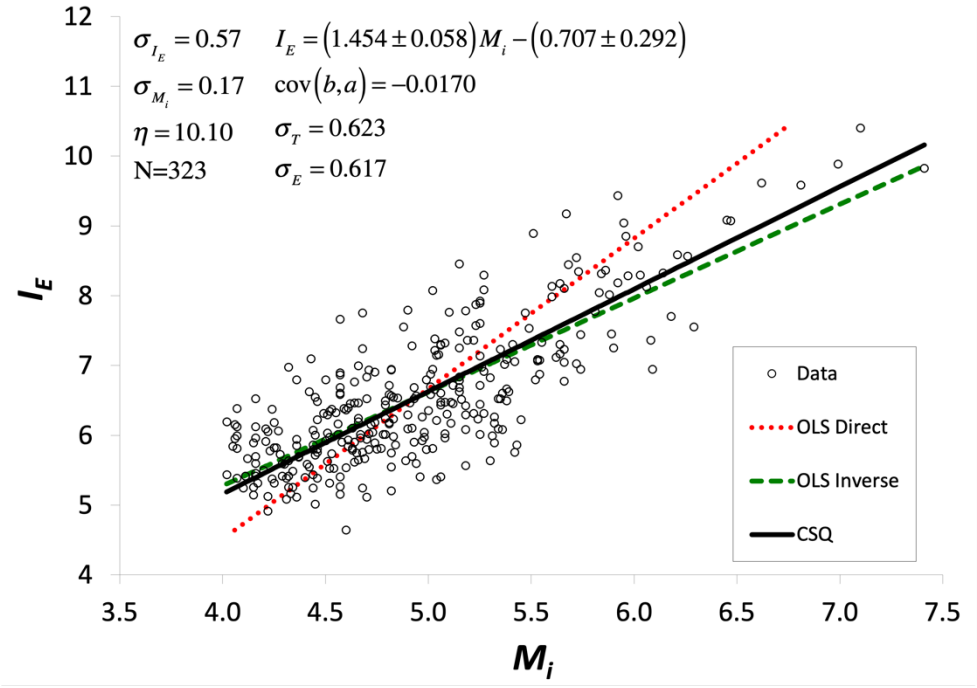

Figure S1 – Regression between I_E and M_i for earthquakes with $M_i \neq 0$

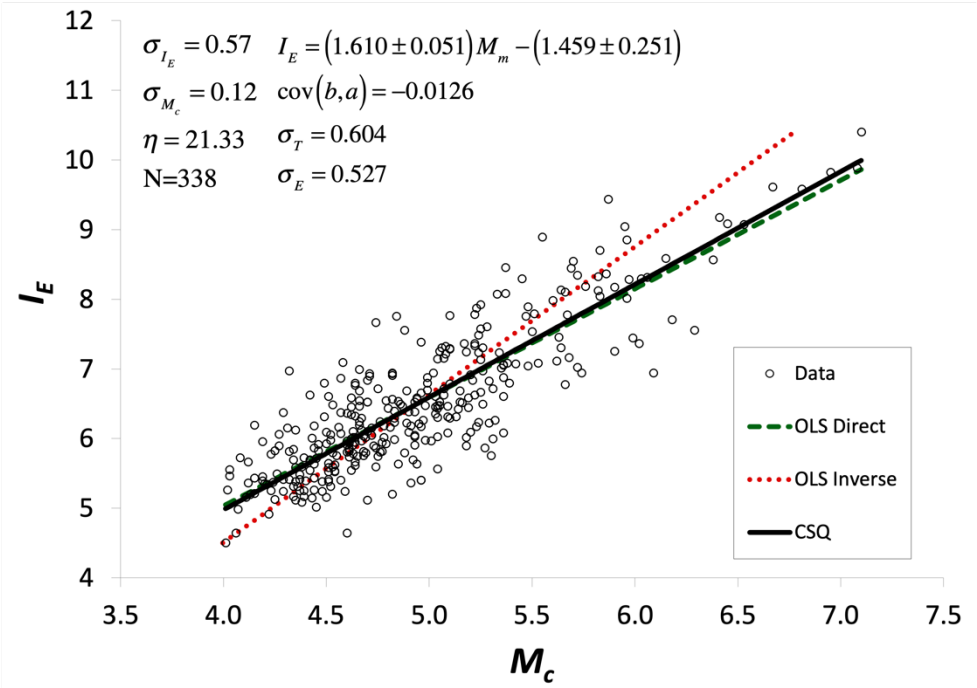

Figure S2 – Regression between I_E and M_c for earthquakes with $M_i \neq 0$

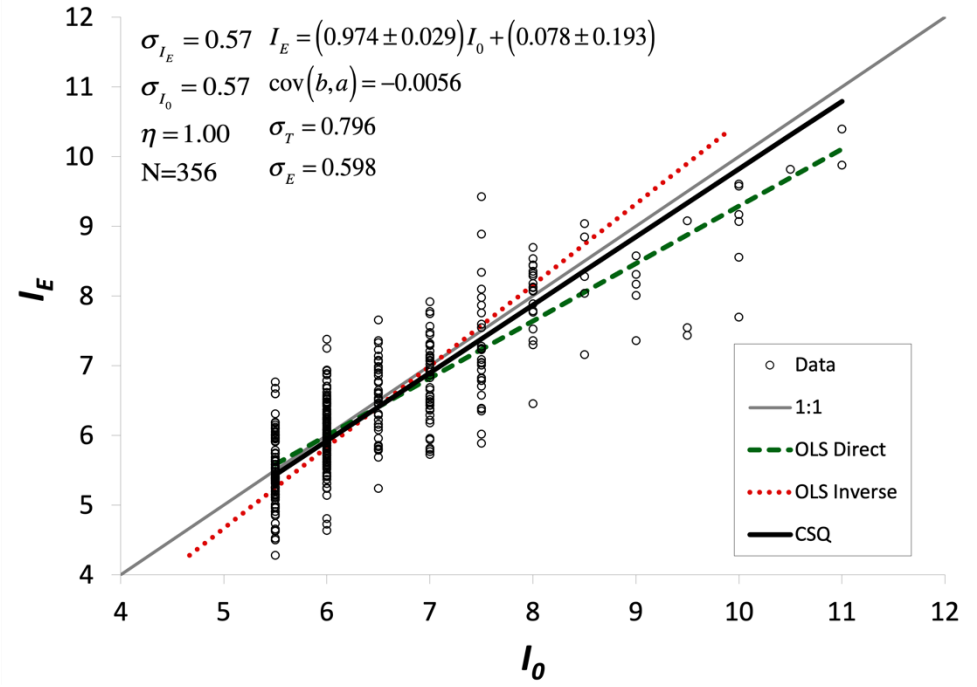

Figure S3 – Regression between I_E and I_0 for earthquakes with $M_i \neq 0$

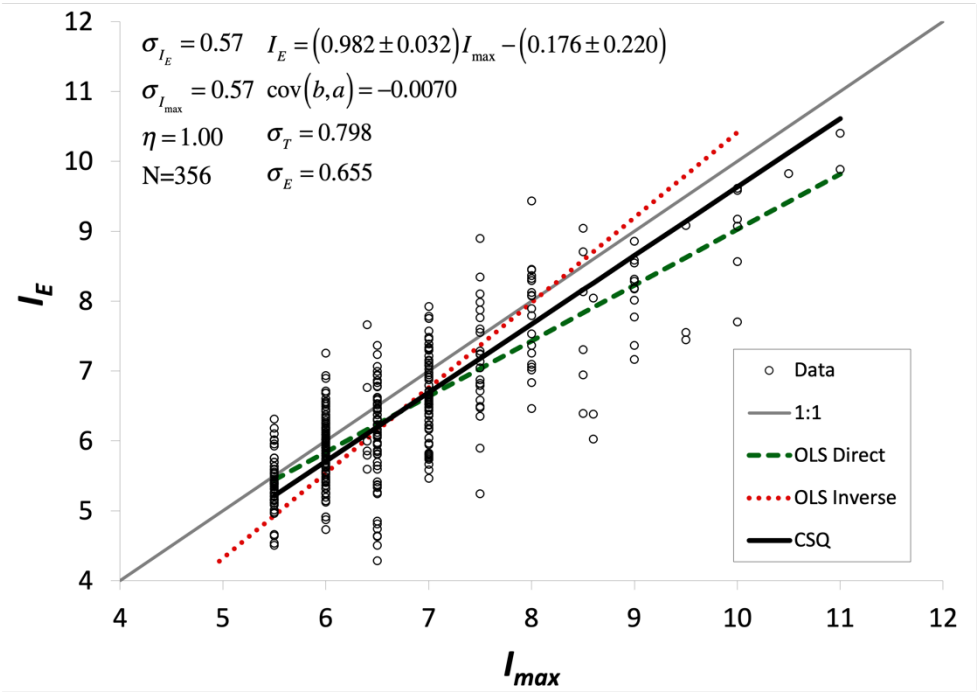

Figure S4 – Regression between I_E and I_{max} for earthquakes with $M_i \neq 0$

Table S1 - for earthquakes with $M_i \neq 0$

Atten. Mod.	*a*	*a'*	*B*	*knee* (km)	*h*(km)	σ	R^2	BIC	AICc
LOGLIN	-0.0066±0.0005	-	-1.235±0.034	-	6.35±0.34	0.626567	0.671654	-21995.1	-21988.0
BILIN	-0.0600±0.0004	-0.0185±0.0002	-	45	0.00±0.29	0.633950	0.663871	-22174.4	-22167.3
LOG	-	-	-1.661±0.016	-	9.54±0.24	0.629138	0.668954	-22051.8	-22046.7
CRAM	-	-	-1.292±0.009	-	2.62±0.24	0.627366	0.670817	-22012.3	-22007.2
LOGBIL	-0.0217±0.0030	-0.0101±0.0009	-0.880±0.080	45	4.77±0.50	0.626246	0.671991	-21991.6	-21982.4

Table S2 – For intensity data ≤2009

Regression	Dataset	*N*	*a*	*b*	*p*(*b*=1)	*σ*	*Δ*	*p*(*Δ*=0)
I_E-M_i	Full	311	-0.571±0.292	1.478±0.059	<0.01	0.60	-	-
I_E-M_c	Full	732	-2.617±0.143	1.879±0.028	<0.01	0.51	-	-
I_E-I_0	Full	753	-0.041±0.126	1.012±0.018	0.51	0.65	-0.04±0.02	0.09
I_E-I_{max}	Full	753	-0.379±0.144	1.023±0.020	0.25	0.71	-0.22±0.03	<0.01
I_E-M_i	M_i≥1960	194	-0.635±0.377	1.511±0.079	<0.01	0.57	-	-
I_E-M_c	M_i≥1960	732	-2.628±0.143	1.881±0.028	<0.01	0.51	-	-
I_E-I_0	M_i≥1960	753	0.041±0.126	1.012±0.018	0.51	0.65	-0.04±0.02	0.09
I_E-I_{max}	M_i≥1960	753	-0.379±0.144	1.023±0.020	0.25	0.71	-0.22±0.03	<0.01

Table S3 – List of earthquakes with macroseismic data added in DBMI15 V3.0 and V4.0

DBMI V	Date-Time	Epicentral area	Reference	MDP	Imax
3.0	2014 01 14 03 43	Isole Eolie	Azzaro et al. (2020a)	20	5
	2017 01 30 09 51	Etna - Versante meridionale	Azzaro et al. (2020a)	9	4
	2017 08 25 21 57	Etna - Versante sud-occidentale	Azzaro et al. (2020a)	6	5
	2018 08 16	Molise	Castellano et al. (2018)	15	5-6
	2018 09 30 17 24	Piano Pernicana	Azzaro et al. (2020a)	5	5
	2018 10 06 34	Versante sudoccidentale	Azzaro et al. (2020a)	44	6-7
	2018 12 26 02 19	Fleri	Azzaro et al. (2020a)	48	8
	2019 06 23 22 43	Provincia di Roma	Arcoraci et al. (2019)	40	5
	2019 12 09 04 37	Mugello	Bernardini et al. (2019)	11	6
4.0	2020 12 22 20 27	Ragusano	D'Amico et al. (2020)	25	5

Table S4 – List of earthquakes with macroseismic data in DBMI15 V2.0 modified in V3.0 and V4.0

Date-Time	Epicentral earea	DBMI15 V2.0	MDP	Imax	DBMI15 V3.0	MDP	Imax
2014 09 25 16 33	Etna - S. Maria la Stella	D'Amico et al. (2014)	20	5	Azzaro et al. (2020a)	22	5-6
2015 12 08 09 28	Etna - Versante nord-orientale	Azzaro et al. (2015)	19	5	Azzaro et al. (2020a)	19	5
2016 02 08 15 35	Monti Iblei	Azzaro et al. (2016)	58	5	Azzaro et al. (2020a)	58	5-6

Table S5 – Mean intensity residuals (observed-computed) as a function of hypocentral distance

Distance (km)	Mean residual	Mean std	N
2.5	0.069325	0.033971	601
7.5	-0.02277	0.010471	4850
12.5	0.044584	0.010722	4287
17.5	0.01643	0.011773	3550
22.5	0.027981	0.012454	3158
27.5	0.004595	0.014752	2370
32.5	-0.00716	0.015807	2107
37.5	-0.03024	0.019048	1571
42.5	-0.01907	0.019752	1417
47.5	-0.03162	0.024707	1054
52.5	-0.01222	0.025472	958
57.5	-0.03433	0.025008	885
62.5	0.012879	0.026885	792
67.5	0.046942	0.029892	661
72.5	0.034024	0.029928	644
77.5	-0.00267	0.032055	563
82.5	0.044267	0.033258	529
87.5	0.019649	0.037491	443
92.5	0.075061	0.0427	307
97.5	0.059817	0.047478	276
102.5	0.071567	0.047971	279
107.5	0.039863	0.050561	238

112.5	0.008321	0.057934	203
117.5	0.033369	0.063838	141
122.5	0.063752	0.075495	131
127.5	0.031956	0.073037	135
132.5	0.011079	0.078153	120
137.5	-0.03755	0.09216	93
142.5	-0.05863	0.093527	87
147.5	0.21122	0.091986	78
152.5	0.061583	0.086803	79
157.5	0.108364	0.110816	71
162.5	-0.00858	0.087136	68
167.5	-0.09844	0.106828	59
172.5	-0.14909	0.106084	66
177.5	-0.01543	0.171693	44
182.5	-0.08453	0.21759	21
187.5	0.17524	0.19568	23
192.5	-0.29975	0.267809	16
197.5	-0.13273	0.199271	17
202.5	-0.08808	0.264023	16
207.5	-0.75351	0.366069	6
212.5	-0.37915	0.274956	10
217.5	0.414514	0.357152	7
222.5	0.442321	0.315233	5
227.5	0.45828	1.977638	2

Table S6 – Mean intensity residuals (observed-computed) as a function of computed intensity

Computed intensity	Mean residual	Mean std	N
3	0.202665	0.048784	229
4	-0.02753	0.010479	4941
5	0.015298	0.007278	9422
6	0.048885	0.008264	7711
7	0.020661	0.009685	5872
8	-0.06935	0.01371	3324
9	-0.0062	0.024613	1222
10	-0.05341	0.050269	294
11	-0.51213	0.226872	20

References

Arcoraci L., Graziani L., Malagnini A., Martini G., Paolini S., Tertulliani A. (2019). QUEST - Rapporto macrosismico sul terremoto del 23 giugno 2019 Mw 3.6 (ML 3.7) in provincia di Roma. Rapporto interno. doi: 10.5281/zenodo.3269202. (in Italian)

Azzaro R., D'Amico S., Scarfì L., Tuvè T. (2015). Rapporto macrosismico sul terremoto etneo del 8/12/2015 ore 10:28 locali. Istituto Nazionale di Geofisica e Vulcanologia (INGV), Osservatorio Etneo, 3 pp., doi: 10.13127/QUEST/2. (in Italian)

Azzaro R., D'Amico S., Mostaccio A., Scarfì L., Tuvè T., 2016. Rilievo macrosismico del terremoto ibleo dell'8 febbraio 2016 - ore 16:35 locali - Relazione. Istituto Nazionale di Geofisica e Vulcanologia (INGV), Catania, 6 pp., doi: 10.13127/QUEST/20160208. (in Italian)

Azzaro R., D'Amico S., Tuvè T., Scarfì L., Mostaccio A., (2020a). Terremoti con effetti macrosismici in Sicilia nel periodo gennaio 2014-dicembre 2018. Quad. Geofis., 160: 1-62, doi: 10.13127/qdg/160. (in Italian)

Bernardini F., Camassi R., Ercolani E. (2019). Rilievo macrosismico per il terremoto del 9 dicembre 2019 in Mugello. Rapporto tecnico QUEST, Istituto Nazionale di Geofisica e Vulcanologia (INGV), Roma, 6 pp., doi: 10.13127/QUEST/20191209. (in Italian)

Castellano C., Del Mese S., Fodarella A., Graziani L., Maramai A., Tertulliani A., Verrubbi V. (2018). Quest- Rilievo Macrosismico per i terremoti del Molise del 14 e 16 agosto 2018. Rapporto interno INGV. doi: 10.5281/zenodo.1405385. (in Italian)

D'Amico S., Giampiccolo E., Tuvè T., Azzaro R. (2020). Rapporto macrosismico preliminare sul terremoto della costa ragusana (Sicilia meridionale) del 22/12/2020 - ore 21:27 locali. Rapporto tecnico QUEST, Istituto Nazionale di Geofisica e Vulcanologia (INGV). https://doi.org/10.13127/QUEST/20201222. (in Italian)